A database of flow and near pressure field signals obtained for subsonic and supersonic jets impinging on a flat or a perforated plate using large-eddy simulations

Mathieu Varé *, Christophe Bogey †
Univ Lyon, CNRS, Ecole Centrale de Lyon, INSA Lyon, Univ Claude Bernard Lyon I,
Laboratoire de Mécanique des Fluides et d'Acoustique, UMR 5509, 69130 Ecully, France

(Updated on September 21, 2022)

The time signals obtained in the flow and near pressure fields of subsonic and supersonic jets impinging on a flat or perforated plate computed by highly-resolved compressible large-eddy simulations (LES) using cylindrical coordinates (r, θ, z) have been stored in a database. As is the case for the data obtained recently for free jets [1], they can be shared with other researchers, upon request by email, to investigate, for instance, the development of turbulent structures and noise generation mechanisms in impinging jets. The jet conditions (Mach and Reynolds numbers, temperature) and nozzle-exit boundary-layer characteristics (thickness, velocity profile, fluctuation level), the LES grid parameters and the recorded signals (nature and location of the variables stored, time duration and sampling frequency) are briefly described in this short note.

I. Nozzle-exit jet flow conditions

A. Subsonic and nearly ideally expanded supersonic jets

1. Subsonic and nearly ideally expanded supersonic jets impinging on a flat plate

Seven isothermal jets at a diameter-based Reynolds number $Re_D = u_j D/\nu = 10^5$, where u_j, $D = 2r_0$, and ν are the jet nozzle-exit velocity and diameter and the kinematic molecular viscosity, and with a peak turbulent intensity of 9% at the nozzle exit have been computed by LES. They impinge on a flat plate located at a distance $L = 8r_0$ from the nozzle and their Mach numbers $M = u_j/c_0$, where c_0 is the sound speed in the ambient medium, vary from 0.6 to 1.3 in order to investigate the effects of the jet velocity on the establishment and the properties of feedback mechanisms between the nozzle and the plate. The jet parameters are gathered in table 1. Results of the simulations are presented in a conference paper [2]. The mesh grid used for all the simulations, noted FPL8, is detailed in section II. The sets of files recorded are presented in section III. The time signals are recorded during a period of $500r_0/u_j$ for the jet at a Mach number of 1.3 and of $1000r_0/u_j$ for the other jets.

2. Jets at a Mach number of 0.9 impinging on a flat or a perforated plate

Four isothermal jets at a Mach number M = 0.9 and a Reynolds numbers $\mathrm{Re}_D = 10^5$ have been simulated using LES. They are characterized by a peak turbulent intensity of 9% at the nozzle-exit. They impinge on a plate located at a distance $L = 6r_0$ from the nozzle. One plate is flat whereas the three other ones are perforated. Three hole diameters h, ranging from $h = D$ to $2.2D$, are considered with the aim of examining the effects of the hole diameter on the properties of feedback loops establishing between the nozzle and the plate. The parameters of the simulations and flow and noise properties of the jets are detailed in a recent paper [3]. The mesh grids used for the LES are referred to as FPM09 for the flat plate case and as PPM09 for the perforated plate case. They are described in section II. The recording times T are equal to $500r_0/u_j$ in all cases.

*Post-doctoral fellow, mathieu.vare@ec-lyon.fr, ORCID iD: https://orcid.org/0000-0002-8315-7470
†CNRS Research Scientist, christophe.bogey@ec-lyon.fr, ORCID iD: https://orcid.org/0000-0003-3243-747X

C. Rocket jets impinging on a flat or a perforated plate

Overexpanded supersonic jets, typical of rocket jets, iminging on a flat or a perforated plate have been computed. They are characterized by an exhaust Mach number $M_e = 3.1$, a Reynolds number $Re_D = 2\times10^5$, an exhaust temperature and pressure $T_e = 2.5T_a$ and $p_e = 0.63p_a$, with T_a and p_a the ambient temperature and pressure, and a peak turbulent intensity between 1 and 1.5% at the nozzle exit.

1. Rocket jets impinging on a flat plate

Four rocket jets impinging on a flat plate have been simulated for a nozzle-to-plate distance L varying between $15r_0$ and $30r_0$ to study the effects of this distance on the upstream sound radiation. They are reported in table 3. The results of the simulations are documented in Varé & Bogey [4]. The four mesh grids used, referred to as FPM31L15, FPM31L20, FPM31L25 and FPM31L30, are presented in section II. The simulation times after the transient period are equal to $1000r_0/u_e$ for the four jets.

2. Rocket jets impinging on a perforated plate

Four jets impinging on a plate with a hole of diameter h varying from $1.33D$ to $4D$ and the corresponding free jet have been simulated to highlight the influence of the hole diameter on the flow and acoustic fields of a rocket jet. The nozzle-to-plate distance L is equal to $30r_0$, as for M31L30. The jet parameters are given in table 3. The results of the LES are detailed in Varé & Bogey [5] The mesh grids for the perforated plate case, noted PPM31, and for the free jet case, noted FJM31, are shown in section II. The recording times are equal to $1000r_0/u_e$ in all cases.

II. Mesh grid parameters

Some characteristics of the mesh grids FPMX_1X_2LYY, PPMX_1X_2 and FJM31 used for the simulations in the radial and axial directions, namely the numbers of points, the grid physical extents and the mesh spacings at specific positions, are provided in table 4. The FP and PP grids are employed for the flat plate and the perforated plate cases, respectively, X_1X_2 indicates the jet Mach number $M = X_1.X_2$ and YY designates the nozzle-to-plate distance $L = YYr_0$. The FJM31 grid is used for the simulation of the free rocket jet. The variations of the radial and axial mesh spacings are shown in figure 1 for the subsonic and ideally expanded jets and in figure 2 for the rocket jets.

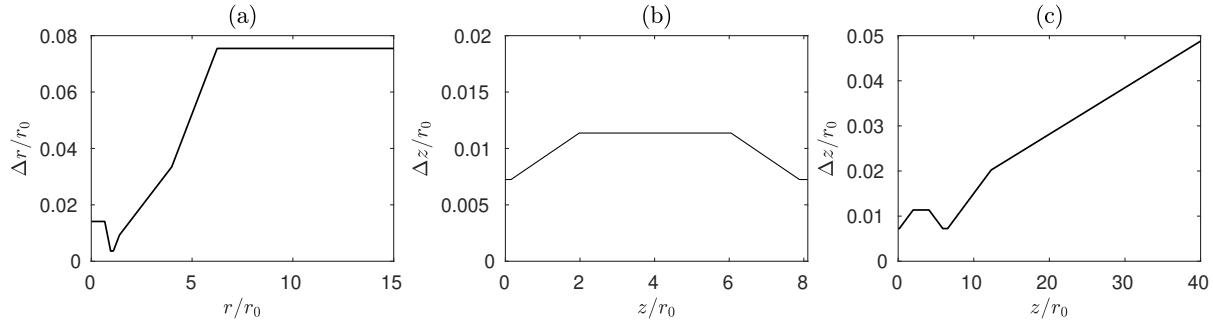

Fig. 1 Variations (a) of radial mesh spacing Δr for FPL8 and PPM09 and of axial mesh spacing Δz for (b) FPL8 and (c) PPM09.

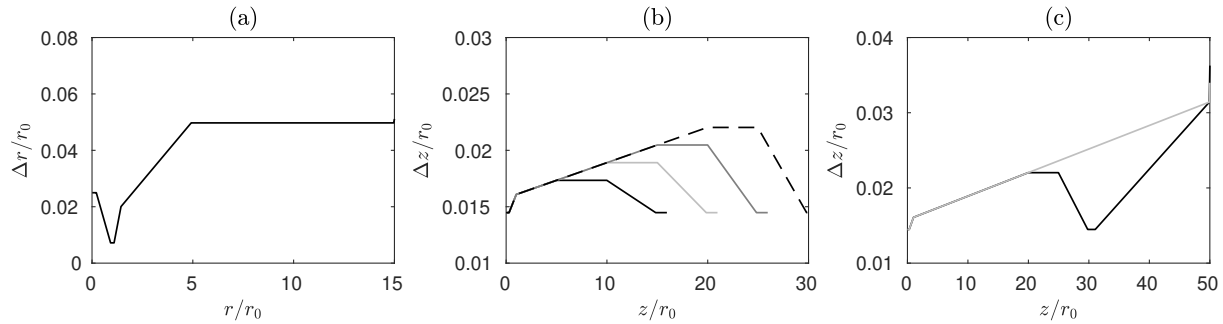

Fig. 2 Variations (a) of radial mesh spacing Δr for FPM31Lxx, PPM31 and FJM31 and of axial mesh spacing Δz for (b) — FPM31L15, — FPM31L20, — FPM31L25 and – – – FPM31L30 and (c) — PPM31 and — FJM31.

III. Recording files

The recording files (nature and location of the variables stored, time durations and sampling frequencies) are defined in table 5. Two-dimensional fields along the jet axis at $r = 0$, along the lip line at $r = r_0$, on the hole edge at $r = h/2$, on the surfaces at $r = 15r_0$, $z = -2r_0$, $z = 0$ and $z = L_z$, and on the plate at $z = L$ and $z = L + e$, where e is the plate width, are stored in the R_0, R_1, R_t, R_{NF}, Z_{start}, Z_0, Z_{end}, Z_{p1} and Z_{p2} files, respectively. Density, the velocity components, pressure are also recorded on four planes at the azimuthal angles $\theta = 0$, 90, 180 and 270 degrees and they are saved in the T_{0-270} files. Their Fourier coefficients up to the mode $n_\theta = 4$ are stored in the $T_{n_\theta=0-4}$ files. The maximum Strouhal number $\mathrm{St}_D = fD/u_j$, where f is the frequency, allowed by the sampling frequency is equal to 6.4 or 12.8.

Acknowledgments

The simulations have been performed using the HPC resources of PMCS2I (Pôle de Modélisation et de Calcul en Sciences de l'Ingénieur et de l'Information) of Ecole Centrale de Lyon, PSMN (Pôle Scientifique de Modélisation Numérique) of ENS de Lyon and P2CHPD (Pôle de Calcul Hautes Performances Dédiés) of Université Lyon I, and the resources of CINES (Centre Informatique National de l'Enseignement Supérieur), IDRIS (Institut du Développement et des Ressources en Informatique Scientifique) and TGCC (Très Grand Centre de calcul du CEA) under the allocations made by GENCI (Grand Equipement National de Calcul Intensif).

References

[1] Bogey, C., "A database of flow and near pressure field signals obtained for subsonic and nearly ideally expanded supersonic free jets using large-eddy simulations," `https://hal.archives-ouvertes.fr/hal-03626787`, 2022.

[2] Varé, M., and Bogey, C., "Mach number dependence of tone generation in impinging round jets," *AIAA Paper 2022-2866*, 2022. https://doi.org/10.2514/6.2022-2866.

[3] Varé, M., and Bogey, C., "Generation of acoustic tones in round jets at a Mach number of 0.9 impinging on a plate with and without a hole," *J. Fluid Mech.*, Vol. 936, 2022, pp. A16 1–32. https://doi.org/10.1017/jfm.2022.47.

[4] Varé, M., and Bogey, C., "Presence and properties of acoustic peaks near the nozzle of impinging rocket jets," *Acta Acustica*, Vol. 6, 2022, p. 36. https://doi.org/10.1051/aacus/2022033.

[5] Varé, M., and Bogey, C., "Flow and acoustic fields of rocket jets impinging on a perforated plate," *AIAA J.*, Vol. 60, 2022, pp. 1–14. https://doi.org/10.2514/1.J061253.

Table 1 LES of subsonic and supersonic ideally expanded jets impinging on a flat plate: see caption of table 2 for the different parameters.

jet	M	Re_D	T_j/T_a	δ_{BL}/r_0	u'_e/u_j	grid	n_θ	L/r_0	Tu_j/r_0
M06L8	0.6	100,000	1	0.15	9%	FPL8	1024	8	1000
M075L8	0.75	100,000	1	0.15	9%	FPL8	1024	8	1000
M08L8	0.8	100,000	1	0.15	9%	FPL8	1024	8	1000
M09L8	0.9	100,000	1	0.15	9%	FPL8	1024	8	1000
M1L8	1	100,000	1	0.15	9%	FPL8	1024	8	1000
M11L8	1.1	100,000	1	0.15	9%	FPL8	1024	8	1000
M13L8	1.3	100,000	1	0.15	9%	FPL8	1024	8	500

Table 2 Mach and Reynolds numbers M and Re_D, jet temperature T_j, thickness δ_{BL} of the boundary-layer profile imposed at the pipe nozzle inlet, peak turbulence intensity u'_e/u_j at the nozzle exit, grid used, number of points n_θ in the azimuthal direction, nozzle-to-plate distance L, hole diameter h and simulation time T after the transient period.

jet	M	Re_D	T_j/T_a	δ_{BL}/r_0	u'_e/u_j	grid	n_θ	L/r_0	h/D	Tu_j/r_0
M09h0	0.9	100,000	1	0.15	9%	FPM09	1024	6	0	500
M09h1	0.9	100,000	1	0.15	9%	PPM09	1024	6	1	500
M09h15	0.9	100,000	1	0.15	9%	PPM09	1024	6	1.5	500
M09h22	0.9	100,000	1	0.15	9%	PPM09	1024	6	2.2	500

Table 3 Exhaust Mach and Reynolds numbers M and Re_D, jet exhaust pressure and temperature p_e and T_e, thickness δ_{BL} of the boundary-layer profile imposed at the pipe nozzle inlet, peak turbulence intensity u'_e/u_j at the nozzle exit, grid used, number of points n_θ in the azimuthal direction, nozzle-to-plate distance L, hole diameter h and simulation time T after the transient period.

jet	M_e	Re_D	p_e/p_a	T_e/T_a	δ_{BL}/r_0	u'_e/u_j	grid	n_θ	L/r_0	h/D	Tu_j/r_0
M31L15	3.1	200,000	0.63	2.5	0.15	$\approx 1\%$	FPM31L15	256	15	0	1000
M31L20	3.1	200,000	0.63	2.5	0.15	$\approx 1\%$	FPM31L20	256	20	0	1000
M31L25	3.1	200,000	0.63	2.5	0.15	$\approx 1\%$	FPM31L25	256	25	0	1000
M31L30	3.1	200,000	0.63	2.5	0.15	$\approx 1\%$	FPM31L30	256	30	0	1000
M31h1	3.1	200,000	0.63	2.5	0.15	$\approx 1\%$	PPM31	256	30	1.33	1000
M31h2	3.1	200,000	0.63	2.5	0.15	$\approx 1\%$	PPM31	256	30	2	1000
M31h3	3.1	200,000	0.63	2.5	0.15	$\approx 1\%$	PPM31	256	30	3	1000
M31h4	3.1	200,000	0.63	2.5	0.15	$\approx 1\%$	PPM31	256	30	4	1000
M31free	3.1	200,000	0.63	2.5	0.15	$\approx 1\%$	FJM31	256	$+\infty$	$+\infty$	1000

Table 4 Numbers of points n_r and n_z and extents of the physical domain L_r and L_z in the radial and axial directions, and mesh spacings Δr and Δz at different positions.

					$\Delta r/r_0$ (%) at			$\Delta z/r_0$ (%) at		
grid	n_r	n_z	L_r	L_z	$r=0$	$r=r_0$	$r=L_r$	$z=0$	$z=15r_0$	$z=L_z$
FPL8	559	1124	$15r_0$	$8r_0$	0.014	0.0036	0.075	0.0072		0.0072
FPM09	559	940	$15r_0$	$6r_0$	0.014	0.0036	0.075	0.0072		0.0072
PPM09	559	2430	$15r_0$	$40r_0$	0.014	0.0036	0.075	0.0072	0.023	0.049
FPM31L15	501	1291	$15r_0$	$15r_0$	0.025	0.0072	0.05	0.014	0.014	0.014
FPM31L20	501	1531	$15r_0$	$20r_0$	0.025	0.0072	0.05	0.014	0.019	0.014
FPM31L25	501	1752	$15r_0$	$25r_0$	0.025	0.0072	0.05	0.014	0.02	0.014
FPM31L30	501	1910	$15r_0$	$30r_0$	0.025	0.0072	0.05	0.014	0.02	0.014
FJM31	501	2628	$15r_0$	$50r_0$	0.025	0.0072	0.05	0.014	0.02	0.033
PPM31	501	2950	$15r_0$	$50r_0$	0.025	0.0072	0.05	0.014	0.02	0.033

Table 5 Recording files: Strouhal number given by the sampling frequency, recording positions, and variables recorded (density ρ, velocity components $u_i = (u_r, u_t, u_z)$, pressure p, vorticity norm $|\omega|$, dilatation Θ).

files	St_D	z	r	θ	variables
R_0	12.8	$-2r_0 \to L_z$ every $2\Delta z$	0	$0 \to 2\pi - 2\pi/256$ every $2\pi/256$	$\rho, u_i, p, \|\omega\|, \Theta$
R_1	12.8	$-2r_0 \to L_z$ every $2\Delta z$	r_0	$0 \to 2\pi - 2\pi/256$ every $2\pi/256$	$\rho, u_i, p, \|\omega\|, \Theta$
R_{NF}	12.8	$-2r_0 \to L_z$ every $2\Delta z$	L_r	$0 \to 2\pi - 2\pi/256$ every $2\pi/256$	ρ, u_i, p
R_t	12.8	$L \to L + e$ every $2\Delta z$	$h/2$	$0 \to 2\pi - 2\pi/256$ every $2\pi/256$	ρ, p
T_{moy}	6.4	$-2r_0 \to L_z$ every Δz	$0 \to L_r$ every Δr		Fourier coef $n_{\theta=0}$ for ρ, u_i, p
T_{0-270}	6.4	$-2r_0 \to L_z$ every Δz	$0 \to L_r$ every Δr	$0 \to 3\pi/2$ every $\pi/2$	$\rho, u_i, p, \partial u_i/\partial\theta$
$T_{n_\theta=0-4}$	6.4	$0 \to L_z$ every $2\Delta z$	$0 \to L_r$ every $2\Delta r$		Fourier coef $n_{\theta=0\to4}$ for $\rho, u_i, p, \|\omega\|, \Theta$
$Z_{0/start/end}$	12.8	$-2r_0, 0, L_z$	$0 \to L_r$ every Δr	$0 \to 2\pi - 2\pi/256$ every $2\pi/256$	ρ, u_i, p
$Z_{p1/p2}$	12.8	$L, L + e$	$0 \to L_r$ every Δr	$0 \to 2\pi - 2\pi/256$ every $2\pi/256$	ρ, p for a flat plate ρ, u_z, p for a perforated plate